10810 *Biochemistry* **2009,** *48,* 10810–10817
DOI: 10.1021/bi901481k

BIOCHEMISTRY
including biophysical chemistry & molecular biology
Article

Engineering Protein Stability and Specificity Using Fluorous Amino Acids: The Importance of Packing Effects[†]

Benjamin C. Buer, Roberto de la Salud-Bea, Hashim M. Al Hashimi, and E. Neil G. Marsh*

Departments of Chemistry, Biophysics, and Biological Chemistry, University of Michigan, Ann Arbor, Michigan 48109

Received August 24, 2009; Revised Manuscript Received October 7, 2009

ABSTRACT: The incorporation of extensively fluorinated, or fluorous, analogues of hydrophobic amino acids into proteins potentially provides the opportunity to modulate the physicochemical properties of proteins in a predictable manner. On the basis of the properties of small fluorocarbon molecules, extensively fluorinated proteins should be both more thermodynamically stable and self-segregate through "fluorous" interactions between fluorinated amino acids. We have examined the effects of introducing the fluorous leucine analogue L-5,5,5,5′,5′,5′,-hexafluoroleucine (hFLeu) at various positions within the hydrophobic core of a de novo-designed four-α-helix bundle protein, α_4. The stabilizing effect of hFLeu is strongly dependent on the positions at which it is incorporated, with per-residue $\Delta\Delta G^{o}_{(fold)}$ ranging from −0.09 to −0.8 kcal mol^{-1} residue^{-1}. In particular, incorporating hFLeu at all the "a" positions or all the "d" positions of the hydrophobic core, thereby creating an alternating packing arrangement of leucine and hFLeu, leads to very stably folded proteins that exhibit higher per-residue $\Delta\Delta G^{o}_{(fold)}$ values than proteins that are packed entirely with hFleu. We conclude that efficient packing of the fluorous amino acid within the hydrophobic core provides a more important contribution to enhancing protein stability than do fluorocarbon−fluorocarbon interactions between fluorinated protein side chains.

The extreme hydrophobicity and low polarizability of perfluorocarbon molecules render them poorly soluble in both polar solvents such as water and apolar solvents such as hexane, a phenomenon known as the fluorous effect (*1*−*4*). This property has been exploited to great effect in the development of methods for purifying organic compounds by tagging them with perfluorocarbon "tails" that allow molecules to be selectively extracted from reaction mixtures into perfluorocarbon solvents (*1*, *3*).

Much interest has focused on whether unusual properties of simple perfluorocarbons can be engineered into proteins by incorporation of extensively fluorinated analogues of hydrophobic amino acids into their structures (*4*−*7*). In particular, fluorination is predicted (a) to confer a general increase in the thermodynamic stability of folded proteins, because fluorocarbon side chains are more hydrophobic than their hydrocarbon counterparts, and (b) to confer self-segregating properties on proteins in which the hydrophobic core is packed with fluorous side chains, by analogy with the self-segregating properties of hydrocarbon and fluorocarbon solvents (*2*, *5*).

The first prediction has proven to be true in many cases, based on studies of a number of peptides designed to adopt α-helical coiled-coil structures that incorporate fluorinated analogues of leucine and valine at "a" and "d" positions of the canonical coiled-coil heptad repeat (*8*−*16*). However, it should be noted that there are exceptions to this prediction. One study found that the intrinsic helix-forming propensities of several fluorinated amino acids were actually lower than that of their nonfluorinated counterparts (*17*). Experiments with the independently folded headpiece subdomain of chicken villin protein found that substituting pentafluorophenylalanine for phenylalanine was either stabilizing or destabilizing, depending upon the position (*18*). In contrast, a recent study on the effect of introduction of tetrafluorophenylalanine into this same protein found large stabilizing effects (*19*). Other experiments have examined the spatial demands of various fluorinated amino acids (*20*). All of these studies serve to emphasize the importance of packing effects in determining the stability of proteins, which are changed to a certain degree by fluorination.

With regard to the second prediction, there is some evidence that fluorinated side chains, incorporated at the hydrophobic interface between helices, can mediate the specific self-association of α-helical peptides in solution (*8*) and in the context of membrane-spanning α-helical peptides (*21*, *22*). However, a recent study in our laboratory that used ^{19}F NMR to investigate the interaction between two four-α-helix bundle proteins, one packed with leucine and the other with 5,5,5,5′,5′,5′-hexafluoroleucine (hFLeu)[1] at the "a" and "d" positions, concluded that the fluorinated and nonfluorinated peptides did not form exclusive interactions (*23*).

We have previously described the design of a model antiparallel four-α-helix bundle protein designated α_4, in which all six layers of the hydrophobic core can be packed with combinations of leucine and hFleu at the buried "a" and "d" positions of the canonical heptad repeat (*15*, *16*). Using this model protein, we investigated the effects of increasing fluorine content by packing two, four, or six layers of the hydrophobic core with hFLeu (*16*). In this paper, we have investigated the effect on protein stability

[†]This research was funded by National Science Foundation Grant CHE 0640934.

*To whom correspondence should be addressed. Telephone: (734) 763-6096. Fax: (734) 615-3790. E-mail: nmarsh@umich.edu.

[1]Abbreviations: hFLeu, L-5,5,5,5′,5′,5′-hexafluoroleucine; CD, circular dichroism; TFA, trifluoroacetic acid; GuHCl, guanidinium chloride.

 Published on Web 10/13/2009

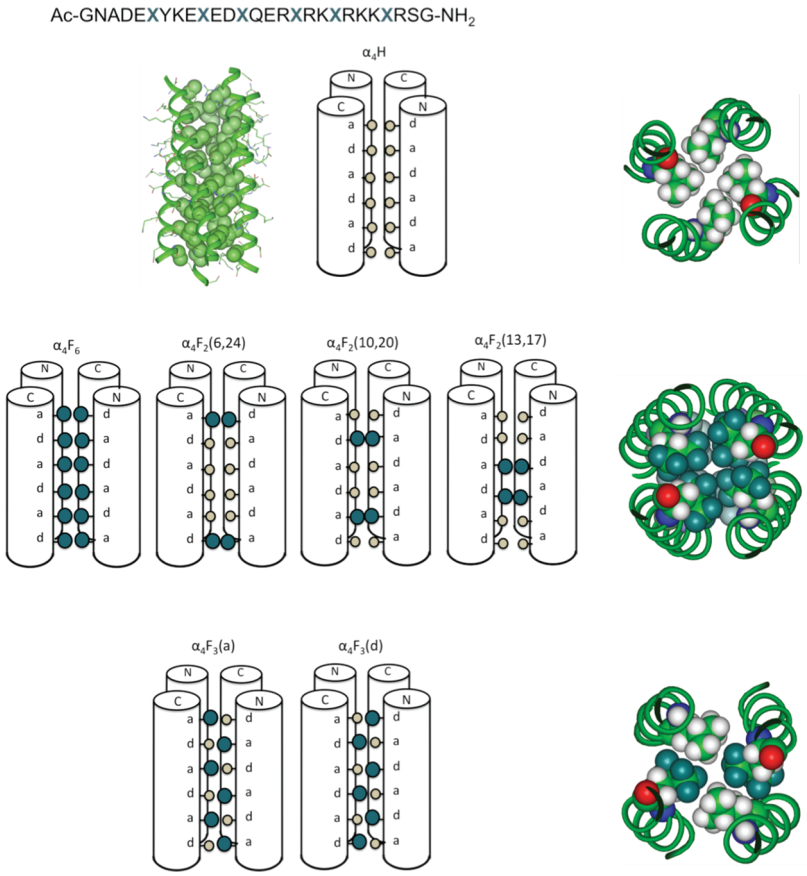

FIGURE 1: Design of the peptides used in this study. The top panel shows the sequence of the α_4 series of peptides where X is either Leu or hFLeu. Models of α_4H illustrate the packing of Leu (represented as space-filling spheres) in the hydrophobic core of the entire protein and one layer of the antiparallel four-helix bundle. The middle panel shows cartoons illustrating the pattern of fluorinated residues packing the hydrophobic core of α_4F_6, $\alpha_4F_2(6,24)$, $\alpha_4F_2(10,20)$, and $\alpha_4F_2(13,17)$ and, at the right, a model illustrating the packing arrangement of four hFLeu side chains within one layer of the hydrophobic core. The bottom panel shows cartoons illustrating the pattern of fluorinated residues packing the hydrophobic core of $\alpha_4F_3(a)$ and $\alpha_4F_3(d)$ and, at the right, a model illustrating the packing of alternating Leu and hFLeu residues within one layer of the hydrophobic core (hFLeu is represented by large green spheres, and Leu is represented by small gray spheres).

of introducing hFLeu residues at different positions within the hydrophobic core while maintaining the same total number of residues within the four-helix bundle. We have also examined the interaction of various combinations of peptides with each other. We conclude that the fluorous effect, as originally envisioned, does not appear to be primarily responsible for the self-segregating properties observed with some of the peptides we have investigated. Rather, a favorable packing arrangement that disperses Leu residues at "a" positions between hFLeu residues at "d" positions (or vice versa) within the hydrophobic core results in a particularly stably folded protein.

EXPERIMENTAL PROCEDURES

Materials. L-5,5,5,5′,5′,5′-Hexafluoroleucine was synthesized as described previously (*24*) and converted to fmoc- or t-Boc-protected derivatives by standard procedures. The sequences of peptides α_4F_6 and α_4H used in this study are shown in Figure 1. These were synthesized by automated fmoc procedures (α_4H) or manual boc procedures (α_4F_6) as described previously (*15*, *16*).

Circular Dichroism. CD spectra of peptides were recorded with an Aviv 62DS spectropolarimeter at 25 °C. Mean residue ellipticities, [θ], were calculated using eq 1

$$[\theta] = \theta_{obsd}/(10lcn) \quad (1)$$

where θ_{obsd} is the ellipticity measured in millidegrees, c is the molar concentration, l is the cell path length in centimeters, and n is the number of residues in the protein. To examine the unfolding of the peptide by GuHCl, stock solutions were prepared containing 40 μM peptide (concentration of monomer) in 10 mM potassium phosphate buffer (pH 7.0) both with and without 8.0 M GuHCl. An autotitrator was used to mix the two solutions to incrementally increase the concentration of GuHCl in the sample CD cuvette (path length of 1 cm); after equilibration for several minutes, the ellipticity at 222 nm was measured. Where appropriate, the denaturation profiles for the peptides were analyzed assuming a two-state equilibrium between unfolded monomeric peptide and folded, tetrameric bundle, with no significantly populated intermediates being present, as described previously (*15*). Igor Pro (Wavemetrics, Inc.) was used to fit the denaturation curves.

Analytical Ultracentrifugation. Sedimentation equilibrium experiments were performed using a Beckman XLA analytical ultracentrifugation system equipped with scanning UV−visible optics (*25*). The initial peptide concentration was 200 μM in 10 mM potassium phosphate buffer (pH 7.0). The temperature was 293 K. The samples were centrifuged at 35000, 37500, 40000, 42500, and 45000 rpm and were judged to have reached equilibrium when successive radial scans were indistinguishable. The data were fitted to a single species using the Ultrascan software package (B. Demeler, University of Texas Health Science Center, San Antonio, TX). Partial specific volumes were calculated using the method of Cohn and Edsall (*26*); the following partial specific

volumes of the peptides were calculated: 0.74 $cm^3\ g^{-1}$ for α_4H, 0.66 $cm^3\ g^{-1}$ for α_4F_6, 0.71 $cm^3\ g^{-1}$ for α_4F_2, and 0.70 $cm^3\ g^{-1}$ for α_4F_3 (the positional variants of α_4F_2 and α_4F_3 were assumed to each have the same partial specific volumes). The calculated tetramer molecular mass for all α_4F_2 peptides is 14060 Da and that for both α_4F_3 peptides 14490 Da. The experimentally determined molecular masses are all consistent with the peptides forming tetramers: 14300 ± 1000 Da for α_4F_2(6,24), 13400 ± 1000 Da for α_4F_2(10,20), 13400 ± 1000 Da for α_4F_2(13,17), 14500 ± 1000 Da for α_4F_3(a), and 16500 ± 1000 Da for α_4F_3(d). The molecular mass of α_4F_3(d) was slightly higher than that calculated for a tetrameric protein; however, given the errors associated with these measurements, we do not consider this difference to be significant. The α_4H and α_4F_6 peptides have previously been shown to be tetramers (*16*).

^{19}F NMR Spectra. ^{19}F NMR spectra were recorded using a Varian 400 MHz NMR spectrometer equipped with a ^{19}F probe. Peptide samples (0.5−4.5 mM) were prepared in 10% D_2O in a final volume of 0.5 mL and buffered to pH 7.0 with phosphate buffer unless otherwise noted. Spectra were recorded at 25 °C and were referenced to trifluoroacetate ion at 0 ppm.

RESULTS

The parent peptide for these experiments was α_4H (*15*), a 27-residue peptide containing three canonical heptad repeats that is designed to fold into a tetrameric antiparallel four-helix bundle structure as shown in Figure 1. Previously, we have investigated the effects of incorporating increasing numbers of hFLeu residues into α_4H by synthesizing a series of peptides designed to pack progressively more layers of the hydrophobic core with hFLeu (*15*, *16*). These peptides were α_4F_2, which incorporates hFLeu at positions 13 and 17 to pack the central two layers of the hydrophobic core with hFLeu; α_4F_4, which incorporates hFLeu at positions 10, 13, 17, and 20 to pack the central four layers of the core; and α_4F_6, which incorporates hFLeu at positions 6, 10, 13, 17, 20, and 24 so that the entire hydrophobic core comprises fluorinated residues.

For this study, we synthesized four additional peptides to compare the effects of introducing hFLeu at different positions within the hydrophobic core. To be consistent with our previous nomenclature, these peptides are designated α_4F_n(position), where *n* refers to the number of hFLeu residues and their position within the sequence is indicated in parentheses. α_4F_2(6,24) contains hFLeu at the N-terminal "d" position 6 and the C-terminal "a" position 24, so that first and last layers of the hydrophobic core are packed by hFLeu; α_4F_2(10,20) contains hFLeu at the second "a" position 10 and the C-terminal "d" position 20, so that the second and fifth layers of the hydrophobic core are packed with hFLeu. These two peptides were designed to complement α_4F_2(13,17), which we have previously characterized (*15*), and in which the third and fourth layers of the hydrophobic core are packed with hFLeu. We also synthesized two peptides to investigate the effects of introduction of hFLeu at only the "a" positions or at only the "d" positions: α_4F_3(a) contains hFLeu at "a" positions 10, 17, and 24, whereas α_4F_3(d) contains hFLeu at "d" positions 6, 13, and 20. Figure 1 illustrates the arrangement of Leu and hFLeu residues in these various peptides and their packing within the hydrophobic core of the four-helix bundle.

Synthesis and Initial Characterization. All of the fluorinated peptides were synthesized manually using boc chemistry and purified by preparative reverse phase HPLC as described previously. Unless noted otherwise, all the experiments were performed in 10 mM potassium phosphate buffer (pH 7.0). The peptides all exhibited CD spectra with strong minima at 208 and 222 nm; the mean residue ellipticities of the peptides were in the range of 15100−20400 deg cm^2 $dmol^{-1}$ $residue^{-1}$, which are characteristic of extensively helical proteins. We and others have noted previously the variation in mean residue ellipticity that can occur upon incorporation of extensively fluorinated residues into helical peptides (*15*−*17*). We feel it is unlikely that these differences are indicative of significant differences in the secondary structure of the peptides because, for example, the $^{15}N-^{1}H$ HSQC spectrum of α_4F_6 indicates that it is highly structured, even though its mean residue ellipticity is lower than that the more labile α_4H peptide (*16*). The oligomerization state of the peptides was examined by equilibrium analytical ultracentrifugation. The molecular masses determined from the equilibrium sedimentation traces (see Experimental Procedures) were in each case consistent with the peptides adopting a tetrameric structure, as designed.

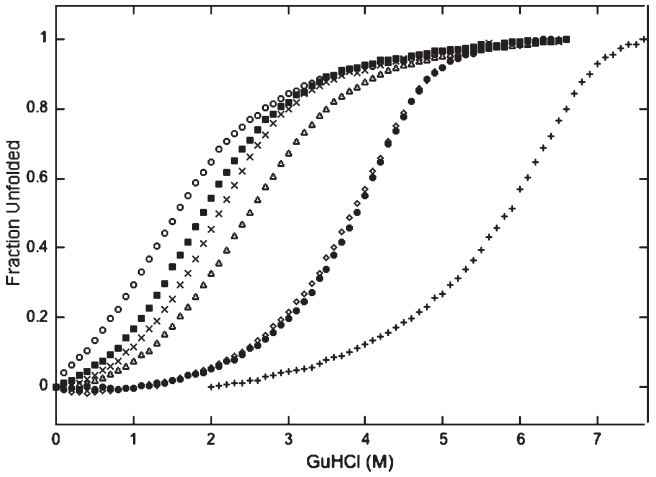

FIGURE 2: Unfolding of peptides in GuHCl. Plots of fraction unfolded vs GuHCl concentration for α_4H (○), α_4F_2(6,24) (■), α_4F_2(10,20) (△), α_4F_2(13,17) (×), α_4F_3(a) (●), α_4F_3(d) (◇), and α_4F_6 (+). Unfolding was followed by measuring changes in ellipticity at 222 nm. The peptide concentration was 40 μM in 10 mM potassium phosphate buffer (pH 7.0) at 25 °C.

Effects of Position on Peptide Stability. The effect on the free energy of folding, $\Delta G°_{(fold)}$, of incorporating hFLeu at different positions within the hydrophobic core of α_4 was investigated by titrating the protein with guanidinium chloride (GuHCl) and monitoring the ellipticity at 222 nm to determine the extent of unfolding. $\Delta G°_{(fold)}$ was determined by fitting the denaturation curves assuming a two-state transition between unfolded monomer and folded tetramer, as described previously (*15*). Previous measurements relied on manual mixing to titrate the peptides with GuHCl; however, in these experiments, we used an autotitrator with the result that we were able to collect significantly more data per unfolding experiment with less experimental error.

The denaturation curves and fits for α_4H, α_4F_2(6,24), α_4F_2(10,20), α_4F_2(13,17), α_4F_3(a), α_4F_3(d), and α_4F_6 are shown in Figure 2 and the values of $\Delta G°_{(fold)}$ and *m* reported in Table 1. All the fluorinated peptides were more stable than the parent α_4H peptide, as would be expected simply from the more hydrophobic nature of the hFLeu side chain. We note that $\Delta G°_{(fold)}$ for α_4F_6 is significantly larger than our previously published estimate for

Table 1: Summary of the Thermodynamic Parameters Determined from GuHCl-Induced Unfolding of Peptides

peptide	ΔG°_{fold} (kcal/mol)	m (kcal mol^{-1} M_{GuHCl}^{-1})	$\Delta\Delta G^\circ_{fold}$[a] (kcal/mol)	$\Delta\Delta G^\circ_{fold}$ (kcal mol^{-1} hFLeu residue^{-1})
α_4H	-18.0 ± 0.2	-1.04 ± 0.04	–	–
$\alpha_4F_2(6,24)$	-18.7 ± 0.1	-1.18 ± 0.03	-0.7 ± 0.2	-0.09 ± 0.03
$\alpha_4F_2(10,20)$	-19.8 ± 0.1	-1.22 ± 0.02	-1.8 ± 0.2	-0.23 ± 0.03
$\alpha_4F_2(13,17)$	-20.1 ± 0.1	-1.53 ± 0.04	-2.1 ± 0.2	-0.26 ± 0.03
$\alpha_4F_3(a)$	-27.6 ± 0.1	-2.47 ± 0.03	-9.6 ± 0.2	-0.80 ± 0.02
$\alpha_4F_3(d)$	-26.6 ± 0.1	-2.24 ± 0.03	-8.6 ± 0.2	-0.72 ± 0.02
α_4F_6	-32.6 ± 0.3	-2.38 ± 0.04	-14.6 ± 0.4	-0.61 ± 0.02
peptide mixtures				
$\alpha_4F_2(6,24)/\alpha_4F_2(10,20)$	-20.0 ± 0.1	-1.37 ± 0.03	-2.0 ± 0.02	-0.25 ± 0.03
$\alpha_4F_2(6,24)/\alpha_4F_2(13,17)$	-19.5 ± 0.1	-1.47 ± 0.04	-1.5 ± 0.02	-0.19 ± 0.03
$\alpha_4F_2(10,20)/\alpha_4F_2(13,17)$	-21.0 ± 0.1	-1.61 ± 0.04	-3.0 ± 0.02	-0.38 ± 0.03

[a] $\Delta\Delta G^\circ_{(fold)}$ values calculated relative to α_4H.

this peptide (*16*); we attribute this to the fact that previous measurements were taken at higher peptide concentrations at which we were unable to determine the upper baseline for the unfolding transition. Typically, this leads to an underestimate of $\Delta G^\circ_{(fold)}$.

For the α_4F_2 series of peptides, it is evident that the position within the hydrophobic core at which hFLeu is introduced does influence the stability of the protein. Thus, the $\alpha_4F_2(6,24)$ variant is only slightly more stable than the parent peptide containing no fluorinated residues. This observation is consistent with the residues at positions 6 and 24 occupying the least well buried positions in the hydrophobic core at the termini of the helical bundle where, even when folded, they are still significantly exposed to solvent. The $\alpha_4F_2(10,20)$ and $\alpha_4F_2(13,17)$ peptides both exhibit similar increases in stability, as would be expected because these positions are fully buried in the hydrophobic core. However, we might have expected the $\alpha_4F_2(13,17)$ variant to have been more stable than $\alpha_4F_2(10,20)$, had favorable "fluorous interactions" between fluorocarbon side chains been operating, because this arrangement allows the two fluorous layers of the core to pack adjacent to each other and maximize fluorine−fluorine contacts, whereas for $\alpha_4F_2(10,20)$, the fluorinated layers are separated by hydrocarbon layers.

^{19}F NMR Studies. To obtain further insights into side chain interactions within the α_4F_2 peptides, we recorded the ^{19}F NMR spectra of the peptides. The fluorine nucleus is very sensitive and exhibits large changes in chemical shift in response to changes in environment, making it an excellent probe for examining interactions between fluorinated residues and adjacent side chains, and dynamic behavior of the peptides (*27*, *28*).

The spectra of the α_4F_2 series of peptides are shown in Figure 3; all the spectra were recorded under identical conditions and chemical shifts referenced to TFA. The spectrum of $\alpha_4F_2(6,24)$ exhibited the sharpest peaks, with all four resonances for the diastereotopic trifluoromethyl groups of the two hFLeu residues clearly distinguished. This is consistent with the hFLeu residues at the ends of the bundle occupying less buried positions and being more mobile. The spectrum of $\alpha_4F_2(10,20)$ exhibits distinctly broader peaks, which is consistent with these residues being packed more tightly within the hydrophobic core and being less mobile.

$\alpha_4F_2(13,17)$, however, exhibits much broader peaks, so that the resonances due to the hFLeu residues at positions 13 and 17 are no longer distinguishable and are shifted upfield of the other two peptides. In part, this may be attributable to the further reduced mobility of the hFLeu residues because two adjacent

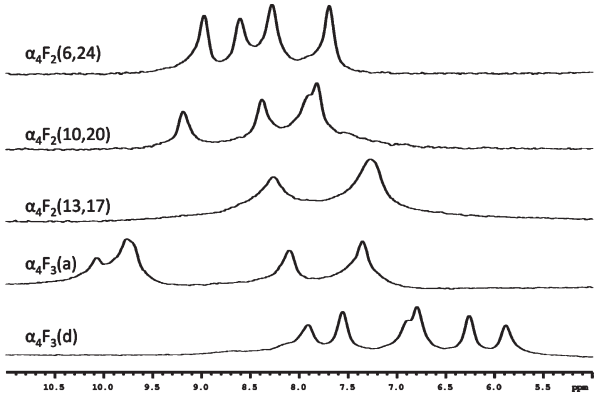

FIGURE 3: ^{19}F NMR spectra of (from top to bottom) $\alpha_4F_2(6,24)$, $\alpha_4F_2(10,20)$, $\alpha_4F_2(13,17)$, $\alpha_4F_3(a)$, and $\alpha_4F_3(d)$ recorded at 25 °C and pH 7.0 in 10% D_2O. All spectra are referenced to TFA.

layers of the hydrophobic core are packed with the more bulky hFLeu side chain. However, we also suspect that part of the broadening may be attributable to the phenomenon of chemical exchange broadening. This would occur if the hFLeu side chains interconverted, on the time scale of micro- to milliseconds, between rotational conformations so that the trifluoromethyl groups sample different chemical environments with different chemical shifts.

Effects of Fluorination at "a" and "d" Positions. Surprisingly, the introduction of hFLeu only at "a" positions, $\alpha_4F_3(a)$, or only at "d" positions, $\alpha_4F_3(d)$, stabilized the proteins by a much greater extent than we expected on the basis of our previous studies of α_4F_2, α_4F_4, and α_4F_6. Furthermore, as one can see in Figure 2, these proteins exhibited a more cooperative unfolding transition [m values significantly increased (Table 1)] indicative of a better packed hydrophobic core. Indeed, the stability of $\alpha_4F_3(a)$ and $\alpha_4F_3(d)$ approaches that for α_4F_6, in which the entire hydrophobic core is fluorinated. The per-residue stabilization afforded by this arrangement of hFLeu side chains is ~3 times greater than that observed in the α_4F_2 series of peptides and ~1.3 times greater than that observed in α_4F_6.

The ^{19}F NMR spectra of $\alpha_4F_3(a)$ and $\alpha_4F_3(d)$ are shown in Figure 3 and are quite distinct; this emphasizes the sensitivity of the ^{19}F nucleus to what are quite subtle differences between the "a" and "d" positions in the hydrophobic core. The spectrum of $\alpha_4F_3(d)$ is somewhat sharper than that of $\alpha_4F_3(a)$, and all six trifluoromethyl groups can be distinguished; for $\alpha_4F_3(a)$, the signals for two of the residues are closely overlapping. Neither spectrum exhibits the pronounced peak broadening seen in the

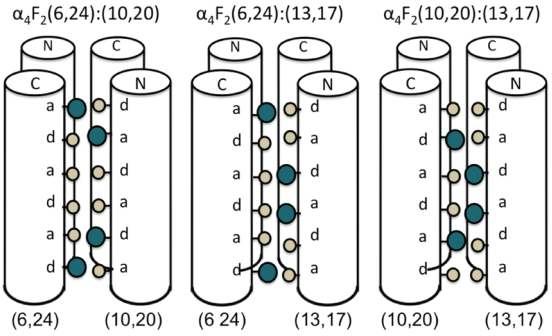

FIGURE 4: Cartoons illustrating the potential packing arrangement of alternating Leu and hFLeu side chains in $\alpha_4F_2(6,24)$:$\alpha_4F_2(10,20)$, $\alpha_4F_2(6,24)$:$\alpha_4F_2(13,17)$ and $\alpha_4F_2(10,20)$:$\alpha_4F_2(13,17)$ heterotetramers (hFLeu is represented by large green spheres, and Leu is represented by small gray spheres).

spectrum of $\alpha_4F_2(13,17)$, implying that the hFleu residues in these proteins are either less restricted in their motion or populate fewer restricted conformations.

It is evident that steric or packing effects (as opposed to simple differences in hydrophobicity) are playing an important role in the stability of $\alpha_4F_3(a)$ and $\alpha_4F_3(d)$. As illustrated in Figure 1, placing hFLeu at "a" positions and Leu at "d" positions (or vice versa) within an antiparallel four-helix bundle results in an arrangement in which hFLeu and Leu residues alternate both within layers and between layers. Notably, this arrangement provides for the maximum dispersion of hFLeu side chains throughout the structure, and thus, the dramatic increase in stability observed for this arrangement is opposite from what would be expected if fluorous interactions between hFLeu residues were important. We suggest that the alternating arrangement of Leu and hFLeu is energetically favorable because it relieves steric crowding, allowing the larger hFLeu residues to be better accommodated within the core of the four-helix bundle.

Stability of Peptide Mixtures. The stability of $\alpha_4F_3(a)$ and $\alpha_4F_3(d)$ provided by the alternate packing of two hFLeu and two Leu residues within the core suggested that the formation of heterotetrameric bundles might be favorable, if the heterotetramer could replicate this packing arrangement. This can potentially be achieved through the formation of heterotetramers of any two of the α_4F_2 peptides, illustrated in Figure 4, which allows for alternate Leu−hFLeu packing of four of the six layers of the core. We therefore mixed together in 1:1 ratios each combination of the α_4F_2 peptides and determined the $\Delta G°_{(fold)}$ values of the mixtures. We expected that if the peptides formed favorable heterotetramers then this should be reflected in the mixtures either unfolding more cooperatively or unfolding at higher concentrations of GuHCl compared to either of the pure peptides. Of course, a statistical mixture of heterotetrameric bundles could arise even if there is no additional stability associated with them, but this would not change the apparent free energy of folding.

The GuHCl denaturation curves for 1:1 mixtures of $\alpha_4F_2(6,24)$ and $\alpha_4F_2(10,20)$, $\alpha_4F_2(6,24)$ and $\alpha_4F_2(13,17)$, and $\alpha_4F_2(10,20)$ and $\alpha_4F_2(13,17)$ were obtained and compared with the denaturation curves that would be expected if the peptides were independently unfolding (i.e., the curve calculated by averaging the two unfolding curves obtained for the pure peptides from data in Figure 2). The apparent $\Delta G°_{(fold)}$ values for these mixtures are given in Table 1. Only the $\alpha_4F_2(10,20)/\alpha_4F_2(13,17)$ mixture exhibited an unfolding transition that occurred at significantly higher GuHCl concentrations compared to that predicted by the calculated curve (Figure 5). Correspondingly, the $\Delta G°_{(fold)}$ calculated for the mixture was significantly larger than that for either of the two pure components, pointing to the formation of more stable heterotetrameric species.

The ^{19}F NMR spectra of the three α_4F_2 peptide combinations were each more complex than those of the individual peptides. Notably, additional resonances, at fields higher and lower than those due to the pure peptides, were observed that can only be attributed to the formation of heterotetrameric species. As noted above, this is to be expected because there are, in principle, six different antiparallel four-helix bundles that can be formed from two peptides, and some heterotetramer combinations may actually be slightly more stable than the corresponding homotetramers. However, the spectra give no indication that the peptide mixtures are assembling into a single, specific heterotetrameric structure, and indeed, this would not be expected in view of the very modest increase in $\Delta G°_{(fold)}$ measured for the peptide mixtures.

We also examined the unfolding of 1:1 mixtures of α_4H and $\alpha_4F_3(a)$, α_4H and $\alpha_4F_3(d)$, and α_4H and α_4F_6. Here the difference in the thermodynamic stabilities of α_4H and $\alpha_4F_3(a)$, $\alpha_4F_3(d)$, or α_4F_6 is very large, so if they formed stable heterotetramers, the unfolding curves of the mixtures should be distinctly different. Whereas we did not expect the α_4H and $\alpha_4F_3(a)$ peptides to form stable heterotetramers, we reasoned that α_4H and α_4F_6 could form a heterotetramer in which each layer of the hydrophobic core was packed with two Leu and two hFLeu residues. This would mimic the alternating packing arrangement that appears to stabilize $\alpha_4F_3(a)$ and $\alpha_4F_3(d)$, although in a hypothetical α_4H:α_4F_6 heterotetramer the hFLeu residues occupy alternating "a" and "d" positions throughout the core, rather than only "a" or only "d" positions. On the other hand, if the introduction of extensively fluorinated residues into the hydrophobic core resulted in self-segregating behavior, this should also be reflected in the unfolding curves of these peptide mixtures.

Figure 6 shows the unfolding transitions of the peptide mixtures, and for the sake of comparison, the calculated unfolding curves for a 1:1 mixture of the pure peptides are superimposed. The $\alpha_4H/\alpha_4F_3(a)$ mixture most closely follows the unfolding curve for the ideal, noninteracting peptide mixture. The fit is less good for the $\alpha_4H/\alpha_4F_3(d)$ mixture, and that of the α_4H/α_4F_6 mixture deviates significantly from the unfolding curve expected if the two peptides were completely self-segregating. However, in none of the cases were the curves characteristic of a two-state unfolding transition of a single species that would be expected if a stable, uniquely folded heterotetramer were being formed. This indicates that these peptides exhibit some preference to self-segregate, but at least in the case of $\alpha_4F_3(d)$ and α_4F_6, there is a significant population of heterotetrameric peptides. For the sake of completeness, we also investigated the unfolding of a 1:1 mixture of $\alpha_4F_3(a)$ and $\alpha_4F_3(d)$. However, these peptides have almost superimposable unfolding curves (Figure 2), and the unfolding curve of the mixture was, unsurprisingly, indistinguishable from those of the pure peptides (data not shown).

To provide further insight into the interactions between α_4H and $\alpha_4F_3(a)$ and $\alpha_4F_3(d)$, we recorded the ^{19}F NMR spectra of these peptides in the presence of α_4H. As the concentration of α_4H increased, some new peaks emerged in the spectra of $\alpha_4F_3(a)$ and $\alpha_4F_3(d)$ and some changes in the chemical shifts of some peaks were apparent. However, the most apparent change was the increased level of broadening of the peaks at higher

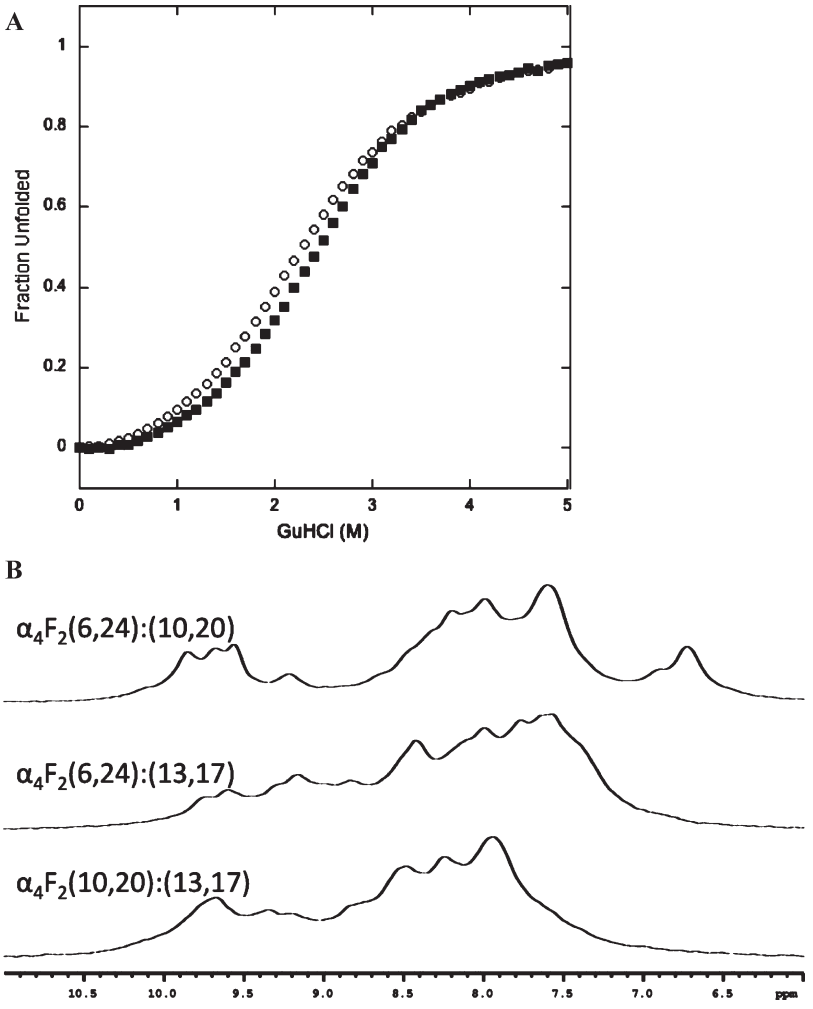

FIGURE 5: (A) GuHCl-induced unfolding of a 1:1 mixture of $\alpha_4F_2(10,20)$ and $\alpha_4F_2(13,17)$ (■) compared to a theoretical unfolding of a 1:1 mixture of $\alpha_4F_2(10,20)$ and $\alpha_4F_2(13,17)$ (○). Conditions are as noted in the legend of Figure 2. (B) ^{19}F NMR spectra of (from top to bottom) $\alpha_4F_2(6,24)$:$\alpha_4F_2(10,20)$, $\alpha_4F_2(6,24)$:$\alpha_4F_2(13,17)$, and $\alpha_4F_2(10,20)$:$\alpha_4F_2(13,17)$ mixtures recorded at 25 °C and pH 7.0.

concentrations of α_4H. Whereas we cannot directly infer the nature of the process underlying the chemical exchange, the broadening observed across different sites is characteristic of having different peptide complexes in chemical exchange with each other on the NMR time scale. We recently published experiments in which we investigated the interaction of α_4H with α_4F_6 by ^{19}F NMR and obtained results qualitatively similar to those described here (*23*).

We note that NMR spectra are very sensitive to the dynamics of peptide folding, and even small changes in the chemical environment and mobility of the ^{19}F nucleus will significantly affect chemical shift and peak shape due to chemical exchange (*29*). In particular, if the peptides undergo exchange between heterotetrameric and homotetrameric species on the NMR (micro- to millisecond) time scale, the spectra will exhibit exchange broadening due to the differences in chemical shifts and relaxation times. If the chemical shift differences are large, as is the case for the fluorine nucleus, an equilibrium population of heterotetrameric species comprising only a few percent would be sufficient to cause significant broadening of the spectra of the homotetramer. Thus, whereas the unfolding experiments point to the presence of at least two large populations of discretely folded peptides with very different unfolding characteristics, the NMR experiments reveal the existence of small subpopulations of heterotetrameric peptides and highlight the dynamic nature of the four-helix bundle structure.

DISCUSSION

Our results show that the incorporation of fluorine into proteins, in this case using hFLeu, can be used as a design strategy to produce very stable proteins. Whereas there is some tendency for these peptides to self-segregate, as predicted by the partitioning of small molecule fluorocarbons into fluorous solvents (*30*) and demonstrated in some other extensively fluorinated de novo-designed peptides (*8*, *21*, *22*), the selectivity is not great. Furthermore, it appears that packing effects within the hydrophobic core are more important than the segregation of fluorinated residues in contributing to the stability of these proteins. Thus, $\alpha_4F_3(a)$ and $\alpha_4F_3(d)$, in which the fluorinated side chains are interspersed with nonfluorinated side chains, exhibit greater per-residue stability than α_4F_6 in which the core is fully fluorinated. The large differences in stability between α_4H and $\alpha_4F_3(a)$, $\alpha_4F_3(d)$, or α_4F_6 appear to provide an adequate explanation for why these peptides prefer to form homotetramers rather than heterotetramers, without the need to invoke fluorous self-segregation per se. Indeed, if anything, α_4F_6 (which is the most stably folded peptide) shows a stronger tendency to interact with α_4H than either $\alpha_4F_3(a)$ or $\alpha_4F_3(d)$.

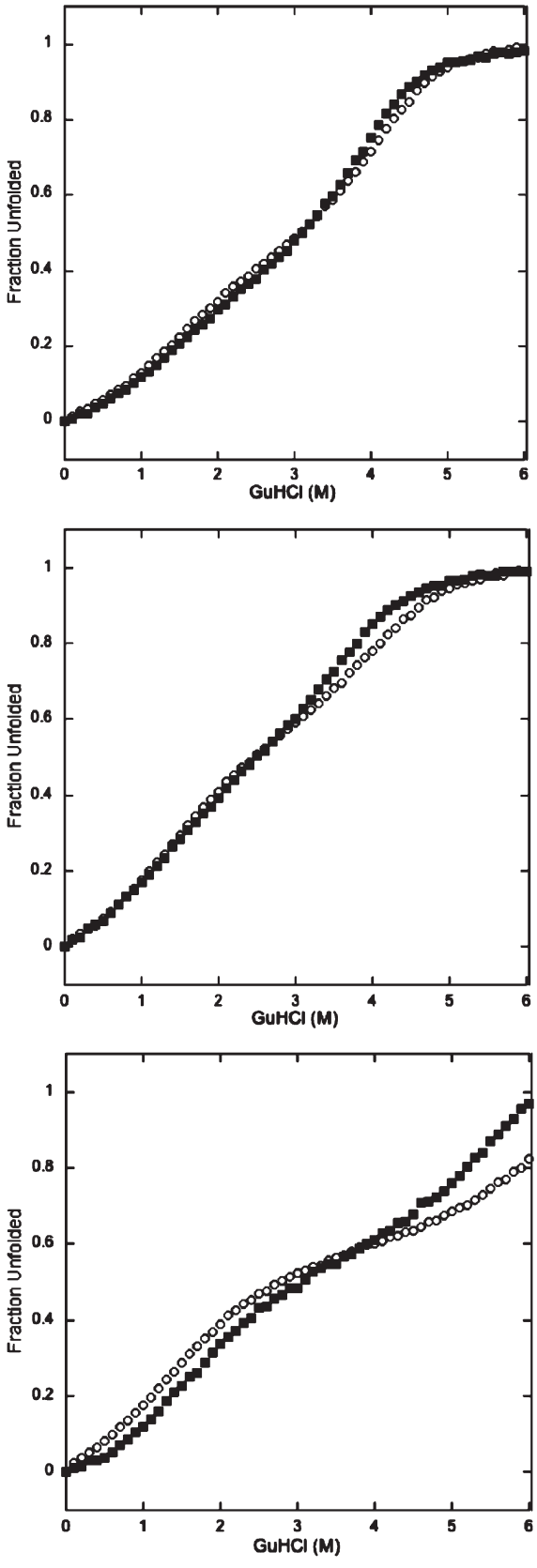

FIGURE 6: GuHCl-induced unfolding of mixtures of fluorinated and nonfluoroinated peptides: (top) 20 μM α_4F_3(a) and 20 μM α_4H, (middle) 20 μM α_4F(d) and 20 μM α_4H, and (bottom) 20 μM α_4F_6 and 20 μM α_4H. For the sake of comparison, the theoretical unfolding curve for a 1:1 mixture of peptides that would result if there were no interaction between peptides is also shown in each case (○). Conditions are as noted in the legend of Figure 2.

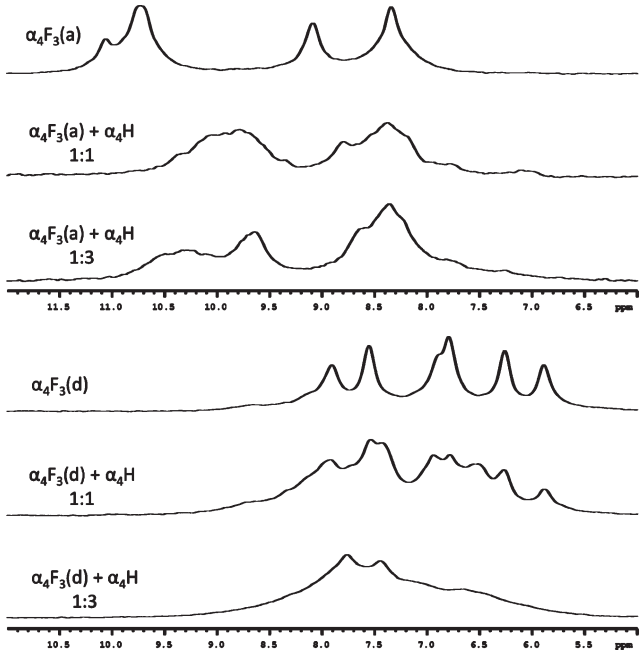

FIGURE 7: ^{19}F NMR spectra of α_4F_3(a) (top) and α_4F_3(d) (bottom) in the presence of increasing concentrations of α_4H. Spectra (from top to bottom) are for 1.5 mM α_4F_3 peptide, 1.5 mM α_4F_3 in the presence of 1.5 mM α_4H, and 1.5 mM α_4F_3 in the presence of 4.5 mM α_4H.

The ^{19}F NMR spectra provide insight into the dynamic behavior of the peptides (Figure 7). Thus, although the fluorinated peptides are thermodynamically very stable, they are also dynamic and the NMR spectra provide evidence of exchange of individual peptides between helical bundles on the micro- to millisecond time scale. The spectra also suggest that packing adjacent layers of the hydrophobic core with hFLeu may result in overpacking of the core of α_4F_2(13,17), resulting in slow interconversion of different side chain conformers that give rise to the broadening of the spectrum. It is worth noting that similarly broad and more complex ^{19}F NMR spectra have previously been observed for α_4F_4 and α_4F_6 peptides (*16*), where the degree of overcrowding of the protein core with hFLeu would be even greater.

These experiments further exemplify the usefulness of fluorine as a label in probing protein−protein interactions, protein structure, and dynamics using NMR. More sophisticated ^{19}F NMR experiments are planned to examine how fluorination modulates the dynamics of these model proteins.

REFERENCES

1. Horvath, I. T., and Rabai, J. (1994) Facile catalyst separation without water: Fluorous biphase hydroformylation of olefins. *Science 266*, 72–75.
2. Marsh, E. N. G. (2000) Towards the non-stick egg: Designing fluorous proteins. *Chem. Biol. 7*, R153–R157.
3. Luo, Z. Y., Zhang, Q. S., Oderaotoshi, Y., and Curran, D. P. (2001) Fluorous mixture synthesis: A fluorous-tagging strategy for the synthesis and separation of mixtures of organic compounds. *Science 291*, 1766–1769.
4. Yoder, N. C., Yuksel, D., Dafik, L., and Kumar, K. (2006) Bioorthogonal noncovalent chemistry: Fluorous phases in chemical biology. *Curr. Opin. Chem. Biol. 10*, 576–583.
5. Yoder, N. C., and Kumar, K. (2002) Fluorinated amino acids in protein design and engineering. *Chem. Soc. Rev. 31*, 335–341.
6. Jackel, C., and Koksch, B. (2005) Fluorine in peptide design and protein engineering. *Eur. J. Org. Chem.* 4483.

7. Smits, R., and Koksch, B. (2006) How C-α-fluoroalkyl amino acids and peptides interact with enzymes: Studies concerning the influence on proteolytic stability, enzymatic resolution and peptide coupling. *Curr. Top. Med. Chem. 6*, 1483–1498.
8. Bilgicer, B., Xing, X. C., and Kumar, K. (2001) Programmed self-sorting of coiled coils with leucine and hexafluoroleucine cores. *J. Am. Chem. Soc. 123*, 11815–11816.
9. Bilgicer, B., Fichera, A., and Kumar, K. (2001) A coiled coil with a fluorous core. *J. Am. Chem. Soc. 123*, 4393–4399.
10. Tang, Y., and Tirrell, D. A. (2001) Biosynthesis of a highly stable coiled-coil protein containing hexafluoroleucine in an engineered bacterial host. *J. Am. Chem. Soc. 123*, 11089–11090.
11. Niemz, A., and Tirrell, D. A. (2001) Self-association and membrane-binding behavior of melittins containing trifluoroleucine. *J. Am. Chem. Soc. 123*, 7407–7413.
12. Tang, Y., Ghirlanda, G., Petka, W. A., Nakajima, T., DeGrado, W. F., and Tirrell, D. A. (2001) Fluorinated coiled-coil proteins prepared in vivo display enhanced thermal and chemical stability. *Angew. Chem., Int. Ed. 40*, 1494–1497.
13. Tang, Y., Ghirlanda, G., Vaidehi, N., Kua, J., Mainz, D. T., Goddard, W. A., DeGrado, W. F., and Tirrell, D. A. (2001) Stabilization of coiled-coil peptide domains by introduction of trifluoroleucine. *Biochemistry 40*, 2790–2796.
14. Bilgicer, B., and Kumar, K. (2002) Synthesis and thermodynamic characterization of self-sorting coiled coils. *Tetrahedron 58*, 4105–4112.
15. Lee, K.-H., Lee, H.-Y., Slutsky, M. S., Anderson, J. T., and Marsh, E. N. G. (2004) Fluorous effect in proteins: *De novo* design and characterization of a four-α-helix bundle protein containing hexafluoroleucine. *Biochemistry 43*, 16277–16284.
16. Lee, H. Y., Lee, K. H., Al-Hashimi, H. M., and Marsh, E. N. G. (2006) Modulating protein structure with fluorous amino acids: Increased stability and native-like structure conferred on a 4-helix bundle protein by hexafluoroleucine. *J. Am. Chem. Soc. 128*, 337–343.
17. Chiu, H. P., Suzuki, Y., Gullickson, D., Ahmad, R., Kokona, B., Fairman, R., and Cheng, R. P. (2006) Helix propensity of highly fluorinated amino acids. *J. Am. Chem. Soc. 128*, 15556–15557.
18. Woll, M. G., Hadley, E. B., Mecozzi, S., and Gellman, S. H. (2006) Stabilizing and destabilizing effects of phenylalanine → F_5-phenylalanine mutations on the folding of a small protein. *J. Am. Chem. Soc. 128*, 15932–15933.
19. Zheng, H., Comeforo, K., and Gao, J. (2009) Expanding the fluorous arsenal: Tetrafluorinated phenylalanines for protein design. *J. Am. Chem. Soc. 131*, 18–19.
20. Jackel, C., Salwiczek, M., and Koksch, B. (2006) Fluorine in a native protein environment: How the spatial demand and polarity of fluoroalkyl groups affect protein folding. *Angew. Chem., Int. Ed. 45*, 4198–4203.
21. Bilgicer, B., and Kumar, K. (2004) De novo design of defined helical bundles in membrane environments. *Proc. Natl. Acad. Sci. U.S.A. 101*, 15324–15329.
22. Naarmann, N., Bilgicer, B., Meng, H., Kumar, K., and Steinem, C. (2006) Fluorinated interfaces drive self-association of transmembrane α helices in lipid bilayers. *Angew. Chem., Int. Ed. 45*, 2588–2591.
23. Gottler, L. M., de la Salud-Bea, R., and Marsh, E. N. G. (2008) The fluorous effect in proteins: Properties of α_4F_6, a 4-α-helix bundle protein with a fluorocarbon core. *Biochemistry 47*, 4484–4490.
24. Anderson, J. T., Toogood, P. L., and Marsh, E. N. G. (2002) A short and efficient synthesis of L-5,5,5,5′,5′,5′-hexafluoroleucine from *N*-Cbz-L-serine. *Org. Lett. 4*, 4281–4283.
25. Harding, S. E., Rowe, A. J., and Horton, H. C. (1992) Analytical Ultracentrifugation in Biochemistry and Polymer Science, The Royal Society of Chemistry, Cambridge, U.K.
26. Cohn, E. J., and Edsall, J. T. (1943) Proteins, Amino Acids and Peptides as Ions and Dipolar Ions, Reinhold, New York.
27. Yu, J. X., Kodibagkar, V. D., Cui, W. N., and Mason, R. P. (2005) F-19: A versatile reporter for non-invasive physiology and pharmacology using magnetic resonance. *Curr. Med. Chem. 12*, 819–848.
28. Gerig, J. T. (1994) Fluorine NMR of Proteins. *Prog. Nucl. Magn. Reson. Spectrosc. 26*, 293–370.
29. Seifert, M. H. J., Ksiazek, D., Azim, M. K., Smialowski, P., Budisa, N., and Holak, T. A. (2002) Slow exchange in the chromophore of a green fluorescent protein variant. *J. Am. Chem. Soc. 124*, 7932–7942.
30. Studer, A., Hadida, S., Ferritto, R., Kim, S. Y., Jeger, P., Wipf, P., and Curran, D. P. (1997) Fluorous synthesis: A fluorous-phase strategy for improving separation efficiency in organic synthesis. *Science 275*, 823–826.